Angular Correlations in the β Decay of ^{8}B: First Tensor-Current Limits from a Mirror-Nucleus Pair

A. T. Gallant,[1,*] N. D. Scielzo,[1] G. Savard,[2,3] J. A. Clark,[3] M. Brodeur,[4] F. Buchinger,[5] D. P. Burdette,[3,4] M. T. Burkey,[1,2,3] S. Caldwell,[2,3,6] J. E. Crawford,[5] A. Czeszumska,[7] C. M. Deibel,[8,9] J. Greene,[3] D. Heslop,[6] T. Y. Hirsh,[10] A. F. Levand,[3] B. Longfellow,[1] G. E. Morgan,[6] P. Mueller,[3] R. Orford,[3,5,†] S. Padgett,[1,‡] N. Paul,[11,§] A. Pérez Galván,[3,∥] A. Reimer,[6] R. Segel,[12] K. S. Sharma,[6] K. Siegl,[11,¶] L. Varriano,[2,3] and B. J. Zabransky[3]

[1]*Lawrence Livermore National Laboratory, Livermore, California 94550, USA*
[2]*Department of Physics, University of Chicago, Chicago, Illinois 60637, USA*
[3]*Argonne National Laboratory, Physics Division, Argonne, Illinois 60439, USA*
[4]*Department of Physics and Astronomy, University of Notre Dame, Notre Dame, Indiana 46556, USA*
[5]*Department of Physics, McGill University, Montréal, Québec H3A 2T8, Canada*
[6]*Department of Physics and Astronomy, University of Manitoba, Winnipeg, Manitoba R3T 2N2, Canada*
[7]*Department of Nuclear Engineering, University of California, Berkeley, California 94720, USA*
[8]*Department of Physics and Astronomy, Louisiana State University, Baton Rouge, Louisiana 70803, USA*
[9]*Joint Institute for Nuclear Astrophysics, Michigan State University, East Lansing, Michigan 48824, USA*
[10]*Soreq Nuclear Research Center, Yavne 81800, Israel*
[11]*Physics Department, University of Notre Dame, Notre Dame, Indiana 46556, USA*
[12]*Department of Physics and Astronomy, Northwestern University, Evanston, Illinois 60208, USA*

(Received 2 September 2022; revised 9 January 2023; accepted 3 April 2023; published 12 May 2023)

We present the first measurement of the α-β-ν angular correlation in the Gamow-Teller β^{+} decay of ^{8}B. This was accomplished using the Beta-decay Paul Trap, expanding on our previous work on the β^{-} decay of ^{8}Li. The ^{8}B result is consistent with the V-A electroweak interaction of the standard model and, on its own, provides a limit on the exotic right-handed tensor current relative to the axial-vector current of $|C_T/C_A|^2 < 0.013$ at the 95.5% confidence level. This represents the first high-precision angular correlation measurements in mirror decays and was made possible through the use of an ion trap. By combining this ^{8}B result with our previous ^{8}Li results, we demonstrate a new pathway for increased precision in searches for exotic currents.

DOI: 10.1103/PhysRevLett.130.192502

Beta-decay measurements were key in establishing the universal vector (V)–axial-vector (A) nature of the electroweak interaction of the standard model (SM) [1,2]. Today, searches for physics beyond the SM (BSM) remain an important topic of theoretical and experimental research. It is expected that BSM physics, such as right-handed neutrinos or supersymmetry [3,4], could manifest as scalar (S), tensor (T), or pseudoscalar (P) currents. The strength of these currents is expressed through the coupling coefficients C_i and C_i', where i can be S, T, A, V, or P, with the terms with primed coefficients being the parity-nonconserving interaction [5]. The existence of exotic S and T currents can be probed in allowed nuclear β decays through their effect on β decay correlations [5,6], such as the β-ν angular correlation coefficient $a_{\beta\nu}$ and the BSM Fierz interference term b_F. In addition, studies with mirror nuclear systems can provide further insights on the underlying β decay physics as several contributions to the decay rate—such as b_F [5] and some of the SM recoil-order terms [7]—change signs for β^{-} and β^{+} decays. This property of recoil-order terms has previously been taken advantage of to explore other symmetries of the SM [8], such as weak magnetism [9,10] and the existence of second-class currents [9,11,12].

Because of the difficulty in detecting the neutrino, the signature of $a_{\beta\nu}$ is determined from the recoil momentum imparted to the daughter nucleus from the emitted β and ν particles. The development of both atom [13,14] and ion traps [15,16] devoted to the study of nuclear beta decay has revolutionized the search for BSM physics due to their ability to directly measure the energy and momentum of the recoiling daughter nucleus [17–22]. Traps are an ideal apparatus for these precision studies as the trapped nuclides are held nearly at rest in a well-localized volume from which the decay products can emerge nearly free from scattering. An additional benefit of ion traps is their ability to trap any element; this was crucial here, allowing the study of mirror decays in detail.

In this Letter, we have employed the Beta-decay Paul Trap (BPT) [15] to perform a measurement of $a_{\beta\nu}$ in the Gamow-Teller (GT) decay of ^{8}B to investigate the possible existence of tensor-current contributions to the electroweak interaction. This Letter builds upon our work in ^{8}Li [20–22] and represents the first time that $a_{\beta\nu}$ has been measured in both nuclei of a mirror-system pair. By studying both members of the mirror-system pair, we have extended our results using the $\tilde{a}_{\beta\nu}$ prescription [23,24] and demonstrate improved limits on the combined C_T and C_T' space.

In both ^{8}Li and ^{8}B, the decay proceeds from a $J^\pi = 2^+$, $T = 1$ ground state to the $J^\pi = 2^+$, $T = 0$ broad 3-MeV excited state in ^{8}Be. Green's function Monte Carlo *ab initio* calculations limit the potential admixture with a Fermi decay to be $\lesssim 0.001$ [25], which is below the sensitivity of this work. The ^{8}Be* immediately breaks up into two α particles, which then differ in energy in the laboratory frame due to the momentum imparted by the emitted leptons.

A detailed measurement of the kinematic shift between the two β-delayed fragments can be used to determine $a_{\beta\nu}$ [26]. The light mass of ^{8}B and the large Q value results in a maximum kinematic shift between the two α particles of $\sim$450 keV in the laboratory frame. To leading order, the decay rate for β-delayed α emission from a nonoriented nucleus is given as [7,27]

$$W \propto F(\pm Z, E_e) p_e E_e (E_0 - E_e)^2 \times \left[g_1 \pm \gamma b_F \frac{m_e}{E_e} + g_2 \frac{\vec{p}_e \cdot \vec{p}_\nu}{E_e E_\nu} + \frac{\tau_{J',J''}(L)}{10} g_{12} \left(\frac{(\vec{p}_e \cdot \hat{p}_\alpha)(\vec{p}_\nu \cdot \hat{p}_\alpha)}{E_e E_\nu} - \frac{1}{3} \frac{\vec{p}_e \cdot \vec{p}_\nu}{E_e E_\nu} \right) \right], \quad (1)$$

where the upper (lower) sign corresponds to β^- (β^+) emission, $F(\pm Z, E_e)$ is the Fermi function, $(E_e, \vec{p}_e)$ and $(E_\nu, \vec{p}_\nu)$ are the four-vectors of the β and ν, respectively, E_0 is the decay end-point energy, m_e is the electron mass, $\hat{p}_\alpha$ is the direction of the emitted α particle, $\tau_{J',J''}(L)$ is a coefficient that depends on the spin sequence $J \to J' \to J''$ of the decay, L is the angular momentum of the α relative to the daughter, and $\gamma = \sqrt{1 - (Z\alpha_{\rm FS})^2}$ with $\alpha_{\rm FS}$ being the fine structure constant. For a pure GT decay, the spectral functions g_i and b_F are dominated by the strength of the A and T currents with small, but important, corrections that arise from recoil-order form factors. In terms of the coupling constants C_T and C_T', and assuming $C_A = C_A'$, $a_{\beta\nu}$ and b_F for GT decays are defined as [5]

$$a_{\beta\nu} = \frac{1}{3} \frac{|C_T|^2 + |C_T'|^2 - 2|C_A|^2}{|C_T|^2 + |C_T'|^2 + 2|C_A|^2}, \qquad b_F = \frac{2{\rm Re}(C_T C_A^* + C_T' C_A^*)}{|C_T|^2 + |C_T'|^2 + 2|C_A|^2}. \quad (2)$$

In this analysis, we first assume a right-handed tensor coupling $C_T = -C_T'$ and later lift this restriction. For these $2^+ \to 2^+ \to 0^+$ $L = 2$ decay sequences, when the α is emitted parallel to the β^+ ($\hat{p}_e \cdot \hat{p}_\alpha = 1$), the effective β-ν angular correlation is enhanced, giving, to leading order,

$$a_{\beta\nu,\rm eff} = \frac{g_2 + (2/3) g_{12}}{g_1} = 3 a_{\beta\nu}, \quad (3)$$

effectively tripling the β-ν angular correlation. Conversely, perpendicular emission ($\hat{p}_e \cdot \hat{p}_\alpha = 0$) effectively suppresses the β-ν angular correlation.

The ^{8}B was produced though the two-proton transfer reaction ^{6}Li(^{3}He, n)^{8}B at the Argonne Tandem-Linac Accelerator System (ATLAS). A 41-MeV beam of ^{6}Li traversed a cryogenic ^{3}He gas target and the reaction products were focused by a large solenoid into a gas catcher. Most of the produced ^{8}B reacted with residual contaminants in the gas catcher and was incorporated into a variety of molecules. This resulted in the activity being spread over many mass units. The peak in ^{8}B activity was located near $A = 42$ with the most likely molecular ion candidate being ^{8}B(OH)$_2^+$. As the lifetime of ^{8}Be* is $\tau \approx 10^{-22}$ s, the beta-delayed, MeV-energy α particles are emitted before the molecular potential can influence the ^{8}Be recoil momentum. Further molecular effects, such as those discussed in Ref. [28], are also negligible. Further details of the production and subsequent stopping, preparation, and injection of the reaction products into the BPT can be found in Refs. [20,29].

The larger mass of the $A = 42$ ions required a retune of the trapping parameters relative to previous measurements that trapped ^{8}Li [20,21]. In order to maximize the trapped ^{8}B population, the axial trapping potential was set slightly shallower than in the previous ^{8}Li measurement, while the radial trapping was provided by a quadrupolar radio frequency (rf) field with $V_{\rm rf} \approx 800 V_{pp}$ and a frequency of 605 kHz. The ions are thermalized by a high-purity helium buffer gas at a pressure of $\sim 10^{-5}$ Torr. The thermalization process is enhanced by circulating liquid nitrogen through the trapping structure, cooling the trap surfaces and He gas to $\sim$90 K. Surrounding the trapping region are four $64 \times 64 \times 1$ mm^3 double-sided silicon strip detectors (DSSDs), with the front and back sides each being segmented into 32 strips. A schematic drawing of the trapping region is shown in Fig. 1. The 1-mm-thick DSSDs allow for both α and β particles to be identified by their energy deposition within a single detector pixel. The β particles typically deposit $\sim$300 keV, although there is a high-energy tail that extends into the region of the α spectrum above $\sim$500 keV. Energy summing between particles is eliminated by requiring distinct pixels for each detected α and β.

Electronic noise, largely arising from rf pickup and dead or damaged strips, led to a large number of strips that had to be excluded from the final analysis. To further reduce noise and the effects of incomplete charge collection, the outmost strips from each detector were excluded from the analysis.

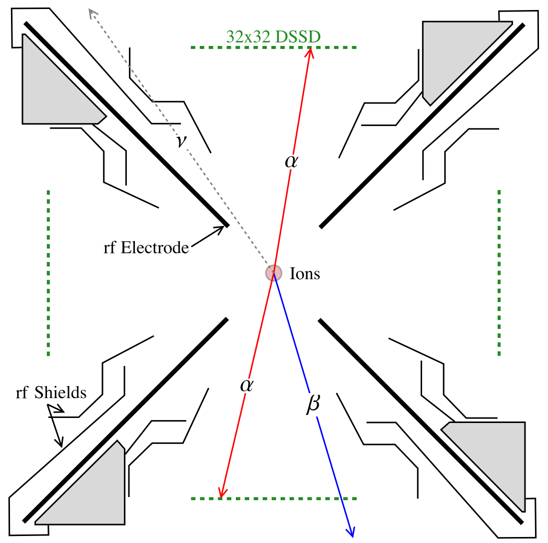

FIG. 1. Cross-sectional view of the BPT and detector system in the rf plane. The directions of the α and β particles are determined by the vectors between the trap center and detector pixels.

This led to the inclusion of 55 front and 57 back strips, or 112 of 128 strips, from the top and bottom detectors, and 30 front and 57 back strips, or 87 of 128 strips, from the left and right detectors in the final analysis.

An average population of ≈ 5 ^{8}B ions was maintained in the BPT during the 6.5 days of data collection, resulting in a total of 6.6×10^5 "double" events and 1.5×10^5 "triple" events, prior to any data cuts. A double event corresponds to opposite facing DSSDs both detecting particles with energies > 740 keV, while a triple event requires the additional detection of a particle with a deposited energy between 200 and 700 keV. Triple events were selected only if (i) more than 35 ms had passed since the last trap closing to allow the ion cloud to thermalize, (ii) two α particles were detected with energies between 740 and 5000 keV and a single β with an energy deposition between 200 and 700 keV, and (iii) the energy difference between the front and back strips was within 45 keV. Radio frequency pickup by the detectors caused clipping in the preamplifier for the highest energy α particles, leading to distortions in the detector response. Minimizing these distortions required placing an upper limit on the detected energy of 5000 keV. The front-back energy cut removes events with incomplete charge collection due to particles hitting the interstrip gap. To account for time-dependent drifts in gain and noise, the data were split into ten segments of ≈ 15 h each.

To fit the data, a comprehensive Monte Carlo simulation suite was developed to simulate the decay kinematics, including the effects from the recoil-order terms [7], electromagnetic corrections [30], induced Coulomb corrections [31], and order-α radiative corrections [32] modified for β-delayed α emission [33]. We use the values of the recoil-order terms from Ref. [10], the Fermi function formulation of Ref. [34] modified for a root-mean-square radius of 2.43 ± 0.24 fm [35], and the excitation energy spectrum of ^{8}Be* following ^{8}B β decay from Ref. [36]. A detailed Autodesk Inventor model of the BPT was developed and exported to a GDML format for use in Geant4. The generated β particles were then passed through Geant4 [37] using the standard electromagnetic physics list "option3," which reproduces the triple events to double events ratio, the backscattered β fractions, and the energy spectrum of the minimum-ionizing β particles in the DSSDs.

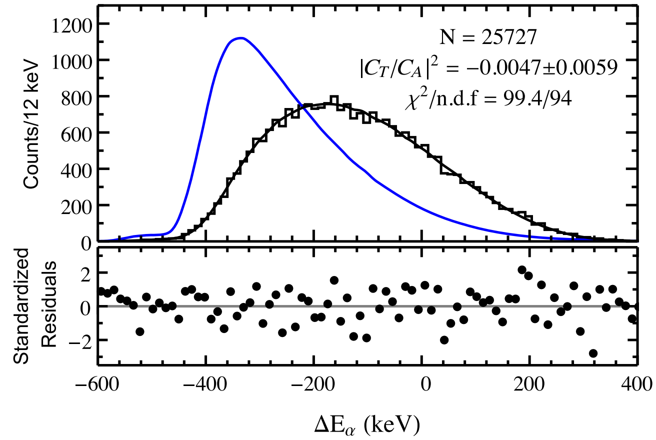

FIG. 2. Energy difference spectrum along with the fit, shown in black, to the simulated spectrum and normalized residuals. Shown in blue is the expected result for a pure tensor interaction. The number of events N, the fitted $|C_T/C_A|^2$, and the fit χ^2 per number of degrees of freedom are also shown.

Simulated spectra for the α energy differences are then generated for pure axial-vector and pure tensor decays for comparison to the experimental data. A linear combination of these simulated spectra are fit to the experimental data, with the ratio of the couplings $|C_T/C_A|^2$ and a normalization constant being the only free parameters. The combined fit of all the detector pairs is shown in Fig. 2 and yields a value of $|C_T/C_A|^2 = -0.0047 \pm 0.0059$.

Many of the systematics affecting our result have been discussed previously [21], and only systematics that have significantly changed for this analysis will be discussed below. All systematic effects for the α energy difference fits at 1σ are listed in Table I.

TABLE I. Dominant sources of systematic uncertainty at 1σ.

Source	$\Delta\lvert C_T/C_A\rvert^2$
Energy calibration	0.0013
α line shape	0.0007
Dead layer thickness	0.0005
Ion-cloud size	0.0005
β scattering	0.0010
Backgrounds	0.0011
Recoil and radiative	0.0048
Nondominant systematics	0.0007
Total	0.0054

Energy calibration and α detector response.—A precision pulser was used to monitor the detector system linearity, and a continuous *in situ* energy calibration was performed using ^{148}Gd and ^{244}Cm sources that emit α particles at 3182.690(24) and 5804.77(5) keV, respectively [38,39]. The largest calibration uncertainty arises from the thick *in situ* calibration sources. These sources were used in [21], and, as in that work, we find that the uncertainty in energy calibration leads to a systematic uncertainty on $|C_T/C_A|^2$ of 0.0013. Charge-collection-dependent effects, such as the detector dead layer, nonionizing energy loss, and pulse height defect were included following Ref. [40]. A high-precision α-energy-response function was developed using data from spectroscopy-grade α sources and accounts for the various detector dead layers and charge sharing between the front and back strips that occurs after an interstrip-gap hit event. Varying the widths of the Gaussian-distributed Fano and electronic noise components of the α-response function lead to an uncertainty on $|C_T/C_A|^2$ of 0.0007, while varying the detector dead layers and nonionizing energy loss lead to an uncertainty on $|C_T/C_A|^2$ of 0.0005.

Ion cloud.—Tuning the trapping electrodes to maximize the number of trapped ^{8}B resulted in a prolate ion cloud. Using the nearly back-to-back α-α coincidences to image the ion cloud [15], the extent of the ion cloud was measured to have full width half maximums of 3.53 mm radially and 6.40 mm axially. We conservatively assume an ion-cloud size uncertainty of $\pm 10\%$, which encompasses both the statistical and systematic uncertainties resulting mainly from missing strips, yielding a systematic uncertainty on $|C_T/C_A|^2$ of 0.0005.

Beta scattering.—In approximately 20% of detected triple events, the β particle scattered prior to reaching a detector. In the energy region of this Letter, the accuracy of the physics models in Geant4 have been extensively tested [41]. Based on this and the results from comparing both the ratio of double to triple events and the fraction of backscattered β events to simulation (see Refs. [21,22]), we estimate the error on β scattering to be 5% and vary the number of scattered events by this amount. This results in a systematic uncertainty on $|C_T/C_A|^2$ of 0.0010.

Recoil and radiative corrections.—Both the ≈1-MeV increase in Q value and the change of sign of some recoil-order form factors between β^+ and β^- decay lead to larger recoil corrections in the decay of ^{8}B relative to the decay of ^{8}Li. The values of the recoil-order terms are from the fitted results of Ref. [10], as the large excitation energy coverage $E_x \approx [1.480, 10]$ MeV necessitates the use of energy averaged recoil-order terms. The state specific calculations for ^{8}Li of Ref. [42] and used in Ref. [22] are not yet available for ^{8}B. The combined correction of d (induced tensor) and b_{WM} (weak magnetism) give rise to an uncertainty on $|C_T/C_A|^2$ of 0.0028. The largest corrections arise from the large uncertainties associated with the second-forbidden j_2 and j_3 terms, leading to a combined uncertainty of 0.0038. The Z-independent radiative corrections, including the effects from bremsstrahlung emission in the final state [32], lead to an uncertainty on $|C_T/C_A|^2$ of 0.0006. The combined uncertainty from the recoil-order and radiative corrections is 0.0048.

Adding the systematic uncertainties in quadrature yields a tensor fraction of

$$|C_T/C_A|^2 = -0.0047 \pm 0.0059_{\mathrm{stat}} \pm 0.0054_{\mathrm{syst}}. \quad (4)$$

A Bayesian analysis with a uniform prior for $|C_T/C_A|^2 > 0$ leads to a limit at the 95.5% confidence level of $|C_T/C_A|^2 < 0.013$ or $|C_T/C_A| < 0.114$. Expressing this in terms of the β-ν angular correlation coefficient results in $a_{\beta\nu} = -0.3365 \pm 0.0039_{\mathrm{stat}} \pm 0.0035_{\mathrm{syst}}$, or $(g_2 + (2/3)g_{12})/g_1 = -1.009 \pm 0.012_{\mathrm{stat}} \pm 0.011_{\mathrm{syst}}$, and are in agreement with the SM predictions of $-1/3$ and -1, respectively. This result is in agreement with our previous results in ^{8}Li of $a_{\beta\nu} = -0.3342 \pm 0.0026_{\mathrm{stat}} \pm 0.0029_{\mathrm{syst}}$ [21] and $a_{\beta\nu} = -0.3325 \pm 0.0013_{\mathrm{stat}} \pm 0.0019_{\mathrm{syst}}$ [22].

In general, it is possible to reinterpret correlation term measurements made under the assumption that $b_F = 0$ (i.e., $C_T = -C'_T$) to include the effect of the Fierz term through the transformation [23,24]

$$\tilde{a}_{\beta\nu} = \frac{a_{\beta\nu}}{1 \pm \gamma b_F \langle m_e/E_e \rangle}, \quad (5)$$

where the upper (lower) sign corresponds to β^- (β^+) emission, $\langle m_e/E_e \rangle$ is the weighted average of E_e^{-1} over the β energy spectrum, and in the present experiment was calculated to be 0.0976.

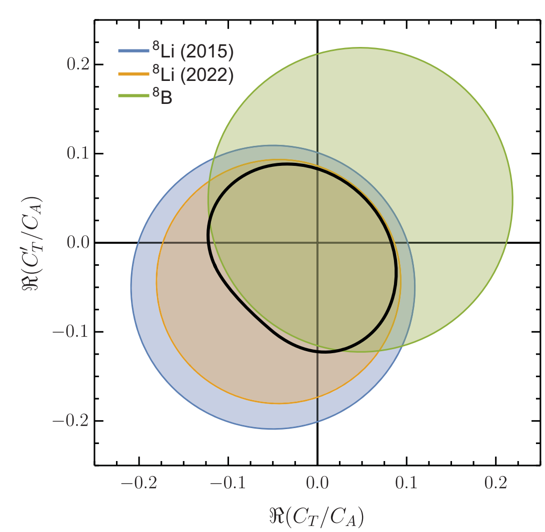

FIG. 3. The 95.5% confidence level regions for ^{8}Li (blue [21], orange [22]), the present ^{8}B measurement (green), and the joint probability distribution (black).

Applying this prescription to our measured $a_{\beta\nu}$ values for $A = 8$, it is possible to construct the probability distributions in (C_T, C'_T) space, as shown in Fig. 3. The change in sign of b_F between ^{8}Li and ^{8}B results in the centers of the $\tilde{a}_{\beta\nu}$ distributions in opposite quadrants in (C_T, C'_T) space, providing much stronger constraints along $C_T = C'_T$ than one would expect from naively combining measurements. Although the present result for ^{8}B is of lower precision than the combined results for ^{8}Li [21,22], the joint probability distribution for $\tilde{a}_{\beta\nu}$ reduces the allowed region by nearly a factor of 2. The high-precision measurement of both mirror systems was only possible through the use of ion traps.

In summary, we have performed the first measurement of the β-ν angular correlation coefficient in the β^+ Gamow-Teller decay of ^{8}B, and the results are in good agreement with the standard model. The largest systematic arises from uncertainties in the recoil-order form factors. The uncertainties can be reduced with future values for ^{8}B with the symmetry-adapted no-core shell model, which has shown great success in the case of ^{8}Li [22,42]. A future joint analysis of higher statistics measurements of ^{8}Li and ^{8}B can be used to further constrain the values of these recoil-order form factors. We have demonstrated a new pathway for increasing the precision of tensor-current searches by employing the $\tilde{a}_{\beta\nu}$ prescription to our results, which is the first time β decay angular correlations have been precisely studied in a mirror-nucleus pair. With a measurement of ^{8}B at a level comparable to Ref. [22], the allowed area in Fig. 3 can further be reduced by nearly 40%.

This work was carried out under the auspices of the U.S. Department of Energy by Lawrence Livermore National Laboratory under Contract No. DE-AC52-07NA27344 and Argonne National Laboratory under Contract No. DE-AC02-06CH11357, and NSERC, Canada, Application No. 216974. M. B. and D. P. B. were supported by the National Science Foundation (NSF) under Grants No. PHY-1713857 and No. PHY-2011890. L. V. was supported by a National Science Foundation Graduate Research Fellowship under Grant No. DGE-1746045. This research used resources of Argonne National Laboratory's ATLAS facility, which is a DOE Office of Science User Facility.

[*]gallant3@llnl.gov
[†]Present address: Lawrence Berkeley National Laboratory, Berkeley, California 94720, USA.
[‡]Present address: Arcfield, Colorado Springs, Colorado 80919, USA.
[§]Present address: Laboratoire Kastler Brossel, Sorbonne Université, CNRS, ENS-PSL Research University, Collège de France, Case 74, 4, place Jussieu, 75005 Paris, France.
[‖]Present address: Vertex Pharmaceuticals, San Diego, California 92121, USA.
[¶]Present address: Department of Physics and Astronomy, University of Tennessee, Knoxville, Tennessee 37996, USA.

[1] R. P. Feynman and M. Gell-Mann, Phys. Rev. **109**, 193 (1958).
[2] E. C. G. Sudarshan and R. E. Marshak, Phys. Rev. **109**, 1860 (1958).
[3] P. Herczeg, Prog. Part. Nucl. Phys. **46**, 413 (2001).
[4] S. Profumo, M. J. Ramsey-Musolf, and S. Tulin, Phys. Rev. D **75**, 075017 (2007).
[5] J. D. Jackson, S. B. Treiman, and H. W. Wyld, Phys. Rev. **106**, 517 (1957).
[6] A. Falkowski, M. González-Alonso, and O. Naviliat-Cuncic, J. High Energy Phys. 04 (2021) 126.
[7] B. R. Holstein, Rev. Mod. Phys. **46**, 789 (1974); **48**, 673 (1976).
[8] L. Grenacs, Annu. Rev. Nucl. Part. Sci. **35**, 455 (1985).
[9] R. E. Tribble and G. T. Garvey, Phys. Rev. C **12**, 967 (1975).
[10] T. Sumikama, K. Matsuta, T. Nagatomo, M. Ogura, T. Iwakoshi, Y. Nakashima, H. Fujiwara, M. Fukuda, M. Mihara, K. Minamisono, T. Yamaguchi, and T. Minamisono, Phys. Rev. C **83**, 065501 (2011).
[11] R. D. McKeown, G. T. Garvey, and C. A. Gagliardi, Phys. Rev. C **22**, 738 (1980).
[12] L. De Braeckeleer, E. G. Adelberger, J. H. Gundlach, M. Kaplan, D. Markoff, A. M. Nathan, W. Schieff, K. A. Snover, D. W. Storm, K. B. Swartz, D. Wright, and B. A. Brown, Phys. Rev. C **51**, 2778 (1995).
[13] J. A. Behr and G. Gwinner, J. Phys. G **36**, 033101 (2009).
[14] J. A. Behr and A. Gorelov, J. Phys. G **41**, 114005 (2014).
[15] N. Scielzo *et al.*, Nucl. Instrum. Methods Phys. Res., Sect. A **681**, 94 (2012).
[16] F. Duval, A. Méry, G. Ban, D. Durand, X. Fléchard, M. Labalme, E. Liénard, F. Mauger, O. Naviliat-Cuncic, D. Rodríguez-Rubiales, and J. Thomas, Nucl. Instrum. Methods Phys. Res., Sect. B **266**, 4537 (2008).
[17] A. Gorelov *et al.*, Phys. Rev. Lett. **94**, 142501 (2005).
[18] P. A. Vetter, J. R. Abo-Shaeer, S. J. Freedman, and R. Maruyama, Phys. Rev. C **77**, 035502 (2008).
[19] X. Fléchard, P. Velten, E. Liénard, A. Méry, D. Rodríguez, G. Ban, D. Durand, F. Mauger, O. Naviliat-Cuncic, and J. C. Thomas, J. Phys. G **38**, 055101 (2011).
[20] G. Li *et al.*, Phys. Rev. Lett. **110**, 092502 (2013).
[21] M. G. Sternberg *et al.*, Phys. Rev. Lett. **115**, 182501 (2015).
[22] M. T. Burkey *et al.*, Phys. Rev. Lett. **128**, 202502 (2022).
[23] H. Paul, Nucl. Phys. **A154**, 160 (1970).
[24] N. Severijns, M. Beck, and O. Naviliat-Cuncic, Rev. Mod. Phys. **78**, 991 (2006).
[25] R. B. Wiringa, S. Pastore, S. C. Pieper, and G. A. Miller, Phys. Rev. C **88**, 044333 (2013).
[26] R. MacFarlane, N. Oakey, and R. Nickles, Phys. Lett. **34B**, 133 (1971).
[27] M. Morita, Phys. Rev. Lett. **1**, 112 (1958).
[28] L. Hayen, N. Severijns, K. Bodek, D. Rozpedzik, and X. Mougeot, Rev. Mod. Phys. **90**, 015008 (2018).
[29] J. Fallis, Ph.D. thesis, University of Manitoba, 2009.
[30] F. P. Calaprice and B. R. Holstein, Nucl. Phys. **A273**, 301 (1976).
[31] B. R. Holstein, Phys. Rev. C **10**, 1215 (1974).
[32] F. Glück, Nucl. Phys. **A628**, 493 (1998).

[33] M. Sternberg, Limits on tensor currents form ^{8}Li β decay, Ph.D. thesis, University of Chicago, 2013.

[34] H. Behrens and J. Jänecke, *Numerical Tables for Beta-Decay and Electron Capture / Numerische Tabellen für Beta-Zerfall und Elektronen-Einfang*, edited by H. Schopper, Landolt-Boernstein—Group I Elementary Particles, Nuclei and Atoms, Vol. 4 (Springer, New York, 1969), 10.1007/b19939.

[35] G. Sargsyan (private communication).

[36] O. S. Kirsebom *et al.*, Phys. Rev. C **83**, 065802 (2011).

[37] S. Agostinelli *et al.*, Nucl. Instrum. Methods Phys. Res., Sect. A **506**, 250 (2003).

[38] Y. A. Akovali, Nucl. Data Sheets **84**, 1 (1998).

[39] B. Singh and E. Browne, Nucl. Data Sheets **109**, 2439 (2008).

[40] T. Hirsh *et al.*, Nucl. Instrum. Methods Phys. Res., Sect. A **887**, 122 (2018).

[41] P. Arce *et al.*, Med. Phys. **48**, 19 (2021).

[42] G. H. Sargsyan, K. D. Launey, M. T. Burkey, A. T. Gallant, N. D. Scielzo, G. Savard, A. Mercenne, T. Dytrych, D. Langr, L. Varriano, B. Longfellow, T. Y. Hirsh, and J. P. Draayer, Phys. Rev. Lett. **128**, 202503 (2022).